

# A Nonparametric Approach for Estimating Three-Dimensional Fiber Orientation Distribution Functions (ODFs) in Fibrous Materials

Adam Rauff, Lucas H. Timmins, Ross T. Whitaker, *Member IEEE*, and Jeffrey A. Weiss

## SUPPLEMENTARY METHODS

### *A. Description of Algorithm*

Images are pre-processed with a Butterworth filter,  $H(x, y, z)$ , prior to the application of our novel technique. The filter serves as the window function to darken the edges of the volume, and results in a spherical volume of analysis. It is parameterized by a cutoff distance  $D_0$  and order  $n$  [43]. The filter,

$$H(x, y, z) = \frac{1}{1 + [D(x, y, z) / D_0]^{2n}}, \quad (1)$$

is also a function of the radial position  $D(x, y, z)$ , where the center of the image is the origin. The cutoff and the order were empirically chosen at 80% of the image radius and  $n = 10$  respectively, assuming a cuboidal image domain.

After solving the Funk-Radon transform using the Qball algorithm, the solution is subject to a post-processing step by a modified min-max normalization [29]. The approximated ODF is composed of a series of harmonic terms, and some ringing effect is expected, particularly for highly anisotropic ODFs. The lower probability values were discarded from the ODF that is outputted from the Qball algorithm,  $\rho_{Qball}$ , by subtracting the minimum probability value,  $\rho_{\min}$ , plus an amount that is proportional to the degree of anisotropy measured by the generalized fractional anisotropy of the ODF retrieved from the Qball algorithm ( $GFA_{Qball}$ ) [29]. The min-max normalization followed the equation

$$\rho = \rho_{Qball} - (\rho_{\min} + (0.1)GFA_{Qball}(\rho_{\max} - \rho_{\min})). \quad (2)$$

The ODFs were then modified to ensure non-negative probability values (Eq. 1 Main Text) by adding the most negative probability value, and the distribution sums to unity (Eq. 2 Main Text) by dividing all probability values by the sum of the ODF (Fig. 2c).

### *B. Statistical Analyses*

*Synthetic Fiber Image Generation.* Synthetic images of fibers were created as Boolean matrices. Each image was 400 cubic voxels, and contained a prescribed number of fibers of length randomly chosen between a user defined minimum and maximum. The direction of each fiber was drawn from a distribution defined by direction along with a standard deviation from the prescribed direction. A fiber was incorporated in the image by randomly selecting a starting point within the middle 300 voxel space. The end-point was found using the fiber length and orientation, and all intermediate

voxels were set to true by sweeping through the point's weighted averages. The image was then dilated using a spherical kernel with a radius of one, and converted to 8-bits.

The exact ODF of the image was constructed by adding a concentrated Gaussian function centered on the direction of each fiber. Initial points on the sphere were obtained using equal-area triangles lying on the unit sphere [1]. As each fiber direction was determined, a Gaussian function was created with standard deviation of two degrees. This function was accumulated over the positive and negative directions along the fiber axis to ensure antipodal symmetry. The exact ODF was then divided by the sum of its area to ensure the probability distribution function constraint. All fiber simulations were conducted in Matlab (Natick, MA, version 2017a).

*Statistical Analyses of ODFs – Riemannian Geometry.* Using the geometric structure on the space of ODFs [2], we could compare a sample of ODFs. This analysis of consistency of the approximation process (Supplementary Fig. 2) necessitated this examination to determine the similarity of a group of approximated ODFs. The mean ODF and its variance were computed from sample of ODFs. The mean ODF is the minimizer of squared distances from every ODFs of the sample. There is no closed form solution to this equation, so an iterative gradient-descent based algorithm was utilized. The variance is then defined as the average of squared distances from the mean ODF. Conceptually, each orientation distribution function was regarded as a vector, and the distance between two vectors is the sum of the tangent vectors in between them. This procedure is analogous to the measurement of length in Euclidean space by integration over velocity between two time points.

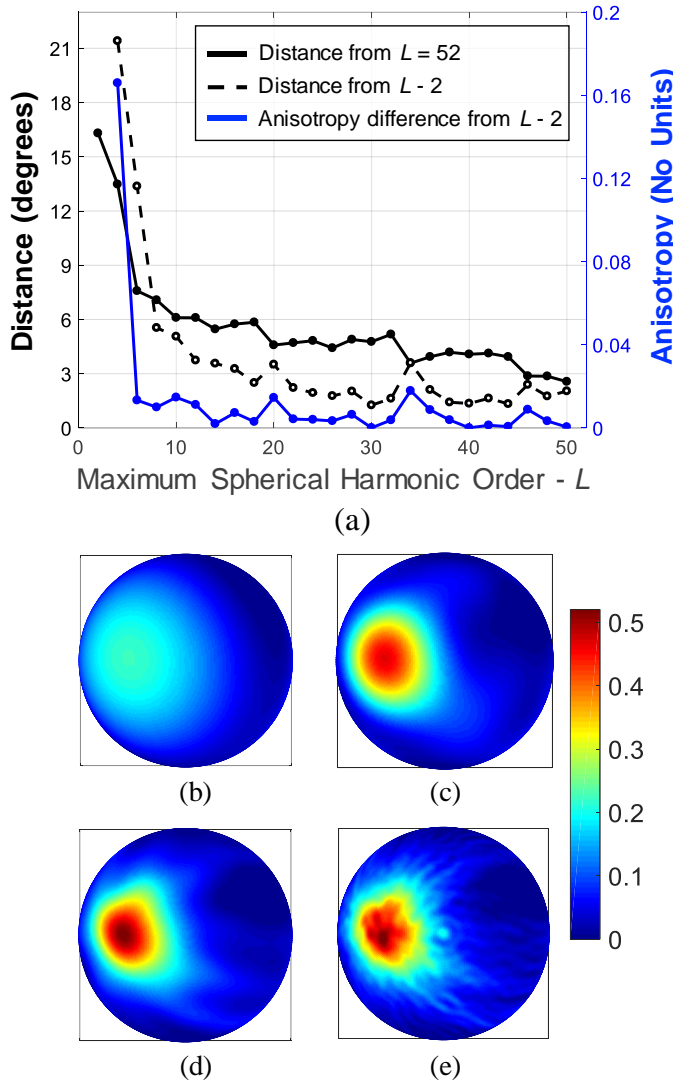
### *C. Verification*

*Harmonic Terms.* The number of spherical harmonic terms used to approximate an ODF is determined manually, yet it affects the angular resolution of the approximated ODFs and the number of scalar terms required to represent it. The effect of the number of harmonic terms was determined by approximating an ODF of biomedical image data using varying number of terms. The ODFs were then compared with the ODF approximation obtained using a high spherical harmonic order.

*Algorithm Precision.* The precision of the approximation process was evaluated empirically by comparing distinct fibrous images with identical fiber orientation distribution functions. The process occurred by choosing an exact ODF, generating multiple synthetic images, approximating each image's ODF, and then comparing the approximated ODFs. The “true” ODF from which simulated fibers were generated were oriented along the x-axis with symmetrical dispersion of  $0^\circ$ ,  $1^\circ$ ,  $2^\circ$ ,  $5^\circ$ , and  $8^\circ$ . Each group included 20 simulated

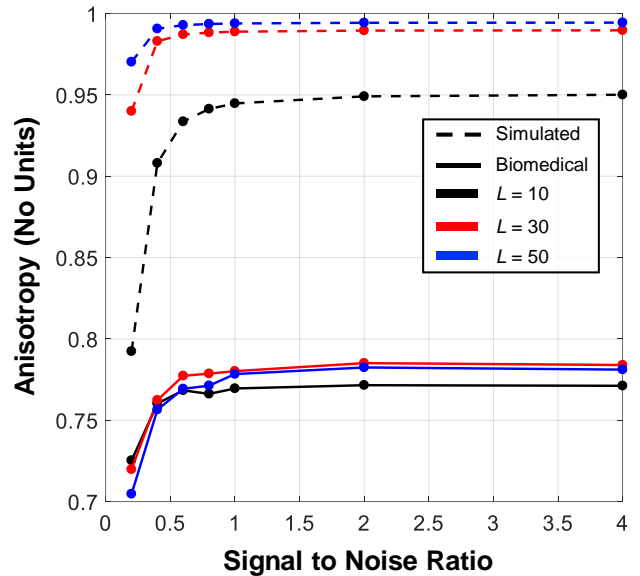
images followed by statistical analysis. Each image contained 300 randomly positioned fibers of length between 10-30% of the image axis length. After conversion to 8bits, each image was blurred using a Gaussian 3 x 3 kernel of with a standard deviation of 10 and added Gaussian noise of a standard deviation of 30. All approximations utilized a maximum spherical harmonic order  $L = 60$ . A mean ODF was then computed from the 20 approximations of each distribution, to determine the deviation of each ODF approximation from the group mean.

### SUPPLEMENTARY FIGURES

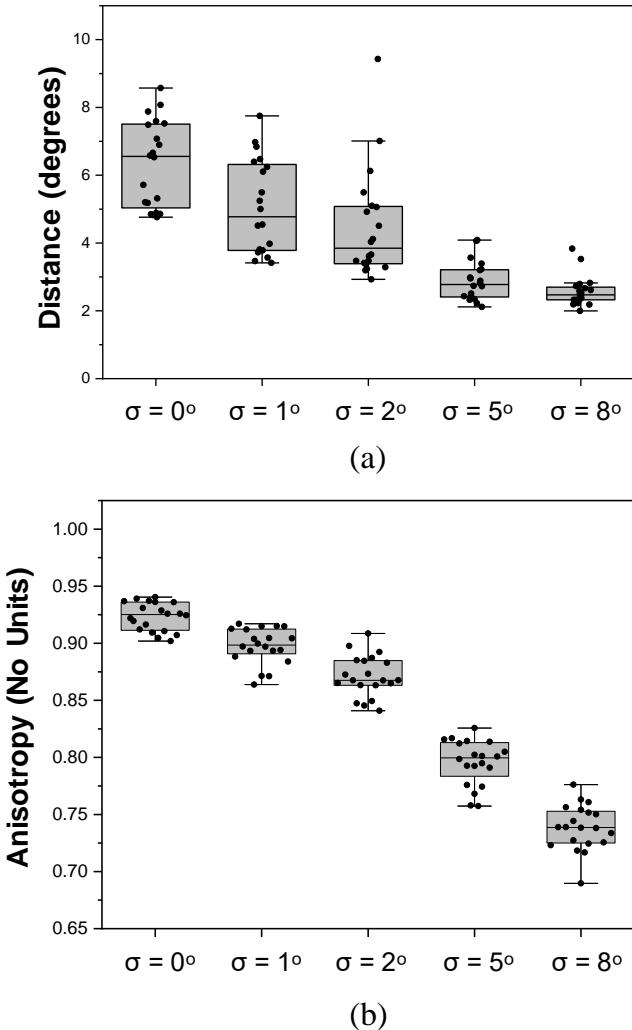


Supplementary Figure 1: The number of harmonic terms used to solve the Funk-Radon transform determines the angular resolution of the ODF. The particular number of spherical harmonic terms will vary from one analysis to another depending on storage requirements and the presence of high frequency content in the underlying, “true,” ODF. The effect of the number of harmonic terms was examined using biomedical image data of actin filaments of a chondrocyte (Fig. 4). Orientation distributions were approximated with varying harmonic order,  $L$ .

Supp. Fig. 1 Continued: The results were compared with an ODF approximated with  $L = 52$  that contains 1431 terms that serves as the high resolution approximation. The ODFs were also compared with the previous harmonic order,  $L - 2$ , to determine how much the distribution was changing as more terms were included (Supp. Fig. 1A). The distance from the high order approximation,  $L = 52$ , decreased from  $16.3^\circ$  at  $L = 2$  to  $7.58^\circ$  at  $L = 6$  and  $5.46^\circ$  at  $L = 14$ . Meanwhile, the distance from the  $L - 2$  approximation decreased from  $21.4^\circ$  at  $L = 4$  to  $13.4^\circ$  at  $L = 6$  and  $5.54^\circ$  at  $L = 8$ . The change in anisotropies rapidly decreased from 0.166 at  $L = 4$  to 0.01 at  $L = 8$ . These quantitative comparisons are intuitively gleaned from the visualizations of the PDFs (Fig. 4b-e) (a) Graph comparing ODF approximations of increasing spherical harmonic order (x-axis). The left y-axis denotes the distance (Methods – statistical Analysis of ODFs). The solid black line represents the distance from the high order approximation,  $L = 52$  (panel e), and the dashed line represents the distance from the  $L - 2$  approximations order. The right y-axis, in blue, represents the anisotropy, and the blue line shows the difference of anisotropy from the  $L - 2$  approximations. (b) Graphical view of ODF approximated with maximum spherical harmonic order  $L = 2$ . The graph is oriented so the x and y axes are in view. (c) ODF approximated with  $L = 6$ . (d) ODF approximated with  $L = 14$ . (e) Highest order ODF approximation with  $L = 52$ .



Supplementary Figure 2: Analysis of the effect of noise on approximated ODFs. The plot exhibits the anisotropy of the ODF approximations at every signal to noise ratio (SNR) that was sampled. Image data were corrupted with varying levels of noise between a minimum of 0.2 to a maximum of 4 SNR. SNR is defined as the ratio of the variance of the noise-free image to the variance of the added noise. The anisotropy was measured using the generalized fractional anisotropy (GFA) for each ODF. Dashed lines remark simulated data, and the solid lines remark biomedical image data. Black curves denote ODF approximation with harmonic order,  $L = 10$ , red curves with  $L = 30$ , and blue curves with  $L = 50$ .



Supplementary Figure 3: Precision of the Algorithm. The precision of the approximation process was assessed by simulating synthetic fiber images from identical underlying ODFs, and comparing the approximations. (a) The Fisher-Rao distance of each approximated ODF from the mean ODF of all approximations. Each group represents 20 simulations of approximated ODFs from simulated fiber images. The distance in units of degrees is graphed on the Y-axis and each group is demonstrated by a box plot overlaid by the scattered data. Every group contained a low variability of measurements that is significantly lower than  $3^\circ$  demonstrating the precision of the measurements. (b) An example of a simulated fiber image that was blurred and corrupted with noise. This image data was simulated from an underlying distribution with symmetrical dispersion of  $\sigma = 8^\circ$ .

## REFERENCES

- [1] A. Semechko, "Suite of functions to perform uniform sampling of a sphere ", ed. GitHub, 2019.
- [2] A. Goh, C. Lenglet, P. M. Thompson, and R. Vidal, "A nonparametric Riemannian framework for processing high angular resolution diffusion images (HARDI)," in *2009 IEEE Conference on Computer Vision and Pattern Recognition*, 2009, pp. 2496-2503.

TABLE 1  
GUIDANCE TO DETERMINE USER-DEFINED VARIABLES

User Determined Variable	Description	Guidance for Use
$D_0$ - Cutoff distance	Pre-processing constant of the Butterworth filter. Determines at what radius, emanating from the center, the image intensity begins to attenuate.	<ul style="list-style-type: none"> <li>• Ensure Butterworth filter removes effect of Fourier assumption of periodic function. Typically manifests in irregular spikes of probability along the direction of the image axes.</li> <li>• Keep consistent for all analyses. We utilized a cutoff of 80% of the image radius.</li> </ul>
$N$ – order	Pre-processing constant of the Butterworth filter. Determines the steepness of the drop off in intensities nearing the image periphery	<ul style="list-style-type: none"> <li>• Ensure Butterworth filter removes effect of Fourier assumption of periodic function. Typically manifests in irregular spikes of probability along the direction of the image axes.</li> <li>• Keep consistent for all analyses. We utilized order <math>n = 8</math>.</li> </ul>
Band-pass filters	Filters used on the power spectrum	<ul style="list-style-type: none"> <li>• Used to exclude components of the image that are not desirable for analysis such as noise and background illumination.</li> <li>• After applying the filter, use an inverse transform to bring signal back to spatial domain of the original image. Observe which features were attenuated as a result of the filtering.</li> <li>• This process should be determined separately for each set of images.</li> <li>• Apply the same filters consistently for samples of the same specimen</li> </ul>
$L$ – Harmonic order	ODF is represented by a sum of harmonic terms extending up to harmonic order $L$	<ul style="list-style-type: none"> <li>• Perform analysis with increasing number of harmonic terms, <math>L</math>. Compare anisotropy and distance with the <math>L - 2</math> approximation (See Supp. Fig. 1).</li> <li>• Choose harmonic order where distance and anisotropy change relatively little. For example, anisotropy changes by less than 0.02 and distance by less than 4° (Supp. Mat. – Figures).</li> <li>• If prior to analysis one knows distribution is highly aligned along a particular direction, or highly concentrated along a few directions, begin with a higher harmonic order (<math>\sim L = 40</math>).</li> <li>• If multiple ODFs are acquired to represent space-varying fiber orientations in a finite-element analysis, use lower harmonic order to keep memory requirements low (<math>\sim L &lt; 20</math>). This guidance will vary with computer hardware.</li> <li>• Effectively limits the number of harmonic terms abled to be used.</li> </ul>
$N$ – ODF Points	Number of points used to sample the ODF	<ul style="list-style-type: none"> <li>• Choose <math>N</math> according to the desired harmonic order and storage requirements.</li> <li>• The sampling of points on the unit sphere will evolve with spherical harmonic decomposition algorithms. For example, we utilized a sampling scheme based on tessellation of triangles, and newer methods utilize iso-latitude rings.</li> </ul>